Soil & Tillage Research 175 (2018) 291–301

Contents lists available at ScienceDirect

Soil & Tillage Research

journal homepage: www.elsevier.com/locate/still

Research paper

Relationships of the hydraulic flow characteristics with the transport of soil organic carbon and sediment loss in the Loess Plateau

L. Liu[a], Z.W. Li[a,b,*], X.F. Chang[a], X.D. Nie[a,b], C. Liu[a,b], H.B. Xiao[a], D.Y. Wang[b]

[a] State Key Laboratory of Soil Erosion and Dryland Farming on the Loess Plateau, Institute of Soil and Water Conservation, CAS and MWR, Yangling, Shaanxi Province 712100, PR China

[b] College of Environmental Science and Engineering, Hunan University, Changsha 410082, PR China

ARTICLE INFO

Keywords:
SOC loss
Soil erosion
Rainfall simulation
Hydraulic characteristics
Transport mechanism

ABSTRACT

Erosive power is characterized by the hydraulic forces of moving water and determines the water transport capacity of soil organic carbon (SOC) and sediment. Understanding the relationships of hydraulic flow characteristics (flow velocity and depth, shear stress and stream power) with the transport of sediments and SOC will improve the understanding of the transport mechanism of sediment and SOC, which in turn will improve SOC prediction. To address this issue, two loess soils (one silt loam and one silty clay) were selected, and 32 simulated rainfall experiments were conducted in a 1 m by 5 m soil pan at a varying slopes (10°, 15°, 20°, and 25°) and two rainfall intensities (90 mm h^{-1} and 120 mm h^{-1}). The results showed that the flow velocities had significant positive linear relationships with the SOC concentrations ($P < 0.001$) under the rainfall intensity of 90 mm h^{-1} and that the flow velocities also had close relationships with the suspension transport of clay particles in the fine-textured soil and the rolling transport of light large aggregates in the coarse-textured soil. Under the rainfall intensity of 120 mm h^{-1}, the runoff depth was positively correlated with the SOC concentrations due to the suspension transport of the clay particles and was negatively correlated with the sediment concentration. The slope had a greater effect on the sediment and SOC loss of the coarse-textured soil than those of the fine-textured soil. Additionally, the stream power was a better descriptor of the sediment loss in the loess soils than shear stress. Overall, both the soil texture and rainfall intensity changed the relationships of the hydraulic flow characteristics with the sediment and SOC loss. Finally, the results of our study will provide important knowledge for improving or building hydraulic-based SOC and sediment loss models.

1. Introduction

Soil erosion always leads to a significant amount of soil organic matter loss (Lal, 2005; Schiettecatteet al., 2008a). The losses of soil and carbon (C) during erosion processes can deplete the fertility of agricultural land and influence atmospheric C circulation (Agata et al., 2015; Gregorich et al., 1998; Kuhn and Armstrong, 2012; Lal et al., 2004; Li et al., 2017; Ma et al., 2016; Williams et al., 1980). Soil erosion disturbs carbon-rich topsoil and preferentially removes soil organic carbon (SOC) from upslope sites, resulting in mineralization as well as the distribution and burial of SOC in depositional environments (Huang et al., 2017; Liu et al., 2017a; Ma et al., 2014; Wang et al., 2014b, 2010; Kuhn et al., 2009; Polyakov and Lal, 2004a). Gaining a better understanding of the removal of SOC due to soil erosion is an important part of elucidating the mechanisms of the SOC cycle (Li et al., 2016a; Liu et al., 2017b; Polyakov and Lal, 2004b). In fact, surface soil erosion is a complicated problem affected by many factors, e.g., microtopography, surface materials and flow characteristics (Fu, 1989). However, the hydraulic forces of moving water and soil types determine the extent of erosion and the transport mechanisms of sediment particles (Slattery and Bryan, 1992; Trout and Neibling, 1993). Flow depth, flow velocity and hydraulic parameters (shear stress, stream power, and unit stream power) are usually used to characterize the erosive power of overland flow determining sediment concentrations (Shih and Yang, 2009). Therefore, it is important to find an analytical solution for the mechanism by which SOC loss is controlled by hydraulic factors.

During the erosion process, if the rainfall energy is large enough and stable, the hydraulic factors, which vary with flow discharges and slope gradients (Schiettecatte et al., 2008b; Shen et al., 2016), control the amount of transported sediment particles (Kinnell, 2005; Shih and Yang, 2009). Previously, stream power was usually used as a measure of the erosive forces associated with the flowing waters for both interrill

* Corresponding author at: State Key Laboratory of Soil Erosion and Dryland Farming on the Loess Plateau, Institute of Soil and Wate Conservation, CAS and MWR, Yangling, Shaanxi Province 712100, PR China.
E-mail address: lizw@hnu.edu.cn (Z.W. Li).

http://dx.doi.org/10.1016/j.still.2017.09.011
Received 18 May 2017; Received in revised form 15 August 2017; Accepted 17 September 2017

Table 1
Selected properties of the original soils from Changwu and Suide.

Property*	Clay (%)	Fine silt (%)	Coarse silt (%)	Sand (%)	MWD (mm)	Bulk density (g cm^{-3})	$CaCO_3$ (g kg^{-1})	SOC (g kg^{-1})	CEC ($cmol_c$ kg^{-1})	pH (in H_2O)
Suide	12.1	19.4	36.3	32.1	0.04	1.25	115.2	2.06	8.1	8.7
Changwu	21.2	38.0	31.3	9.5	0.28	1.20	81.1	6.36	12.4	8.3

MWD: mean weight diameter of aggregates after wet sieving; CEC: cation exchange capacity.
* Soil texture is classified on the basis of the USDA soil classification system.

and rill erosion (Kinnell, 2005; Nearing et al., 1997; Shi et al., 2012). However, flow velocity occasionally has a more significant relationship with sediment transports (Arjmand and Mahmoodabadi, 2015). Hydraulic parameters, e.g., flow velocity, flow depth, stream power and shear stress, are usually used to determine the sediment transport capacity of flow in physics-based erosion models, e.g., the Limburg Soil Erosion Model (LISEM) (De Roo et al., 1996), European Soil Erosion Model (EUROSEM) (Morgan et al., 1998) and Water Erosion Prediction Project (WEPP) (Nearing et al., 1989). SOC loss is mainly understood in term of soil loss (Palis et al., 1997). Although the hydraulic mechanism controlling soil loss has been widely researched (Pan and Shangguan, 2006; Slattery and Bryan, 1992), the relationships of various hydraulic flow characteristics with SOC loss have not been studied, and these relationships are essential for SOC loss prediction.

In previous studies, clay particles, silt particles and light aggregates were the first to be transported during erosion processes (Palis et al., 1997; Rodriguez et al., 2002). These clay and silt particles, which are easily the first to be transported, were strongly correlated with the SOC concentrations (Leifeld et al., 2005; Meersmans et al., 2008; Parton et al., 1987, 1993; Xu et al., 2015). In addition, Moss et al. (1979) noted that sediment particles of different sizes were broadly associated with particular sediment transport modes (e.g. suspended, saltating and contact (rolling) loads). In particular, clay was usually associated with suspension/saltation, whereas large aggregates were transported by rolling (Asadi et al., 2007). Thus, hydraulic forces and soil type determine the sediment transport and sediment size distribution and consequently influence SOC concentration. The SOC concentration related to the selective transport of the sediment, which is controlled by hydraulic factors, needs to be quantified to understand the effects of erosion on the SOC loss in loess soils.

The mechanism of the SOC loss through erosion is determined by three key factors: the distribution of the organic carbon pools in the soil aggregates, the kinetic energy of the rainfall and the structural stability of the soil (Martínez-Mena et al., 2012). For loess soils on the Loess Plateau, soil texture has a considerable effect on the sediment size distribution (Wang and Shi, 2015; Wang et al., 2014a). Hence, this study aimed (i) to analyze the relationships of the hydraulic flow characteristics (flow velocity, runoff depth, stream power and shear stress) with the sediment and SOC loss from the two different soil textures on the Loess Plateau of China and (ii) to determine how the hydraulic factors affect the SOC concentrations due to the selective transport of sediment particles during the erosion process.

2. Methods and materials

2.1. Experimental devices

Simulated rainfall experiments were conducted at the State Key Laboratory of Soil Erosion and Dryland Farming on the Loess Plateau. The down sprinkler rainfall simulator system comprises three nozzles (Shen et al., 2015). The nozzles were placed 18 m above the ground to ensure that the raindrops created in the experiments were similar to natural raindrops. By adjusting the nozzle size and water pressure, rainfall intensities ranging from 30 mm h^{-1} to 350 mm h^{-1} were obtained. The soil pans were constructed with metal sheets measuring 5 m (length) × 1 m (width) × 0.5 m (depth). Each soil pan was electronically adjusted to the proper slope before each experiment. A metal runoff collector was placed at the end of the soil pan to collect the runoff (Shi et al., 2012). Tap water (electrical conductivity = 0.7 dS m^{-1}) was used in all experiments.

2.2. Experimental design

Two loess soil types were selected for this study, one from Suide (37°31′N, 110°16′E) and one from Changwu (35°12′N, 107°47′E), which are distributed in the north and south of the Loess Plateau, respectively. Both of these soil types were sampled from the topsoil (20 cm) of farmland that had been used to cultivate maize (*Zea mays* L.) for several decades. The samples were collected before crop cultivation, when no vegetation was planted in the farmland. The two soils were silt loam and silty clay. The Suide soil had a SOC content of 2.06 g kg^{-1}, whereas the Changwu soil had a SOC content of 6.36 k kg^{-1}. The properties of these soils are shown in Table 1. The climate of the study area is affected by the oceanic monsoon climate and belongs to the subhumid region (Wang and Xiao, 1993; Wei and Shao, 2007). Two rainfall intensities, 90 mm h^{-1} and 120 mm h^{-1}, which represent the typical rainfall intensities of strong storms in the subhumid climatic regions of China, were used in the experiments (Shi et al., 2012; Wang and Shi, 2015). Four typical slope gradients, 10°, 15°, 20°, and 25°, were selected for our study. The slope gradient of 25° is the steepest incline of slope in the region according to the classification of farmland slopes in the Loess Plateau (Comprehensive Scientific Expedition, 1990). A total of 16 treatments were conducted, with two repetitions of each experimental setup.

2.3. Experimental process

Before the experiments, all samples were passed through a 10-mm sieve and mixed thoroughly before being air dried to a 10% moisture content (gravimetric). Before packing the soil, a 10 cm-thick layer of coarse sand was added to the bottom of the experimental soil pan to maintain permeable conditions. Then, a fine gauze was placed on top of the layer of coarse sand. Afterwards, a 30-cm-thick soil layer was placed over the coarse sand layer in 5 cm increments. The Suide and Changwu soil plow layers in the soil pan were packed with bulk densities of 1.25 g cm^{-3} and 1.20 g cm^{-3}, respectively. Each layer was raked lightly to ensure the uniformity and continuity of the soil structure. Prior to performing the experiments, the simulated rainfall device was tested to ensure that it could attain the proper rainfall intensity. The soil surface of the experimental plot was exposed to accept rainfall evenly. During the rainfall process, the runoff and rill initiation times were recorded, and the runoff and soil loss were collected at the outlet once each minute. The rill locations and shapes were frequently measured with a millimeter-scale ruler at numerous points. The changes in sediment transport and soil surface conditions were both visually observed and recorded throughout the erosion process. A fluorescent dye method was used to measure the flow velocity (Gilley et al., 1990). The time for the tracer to travel from the injection point to a downslope point was measured visually. The surface velocity of the overland flow was obtained by dividing the travel distance by the travel time. The flow velocities were measured over a distance of 50 cm successively at four locations within the plot: 75–125, 175–225, 275–325, and 375–425 cm

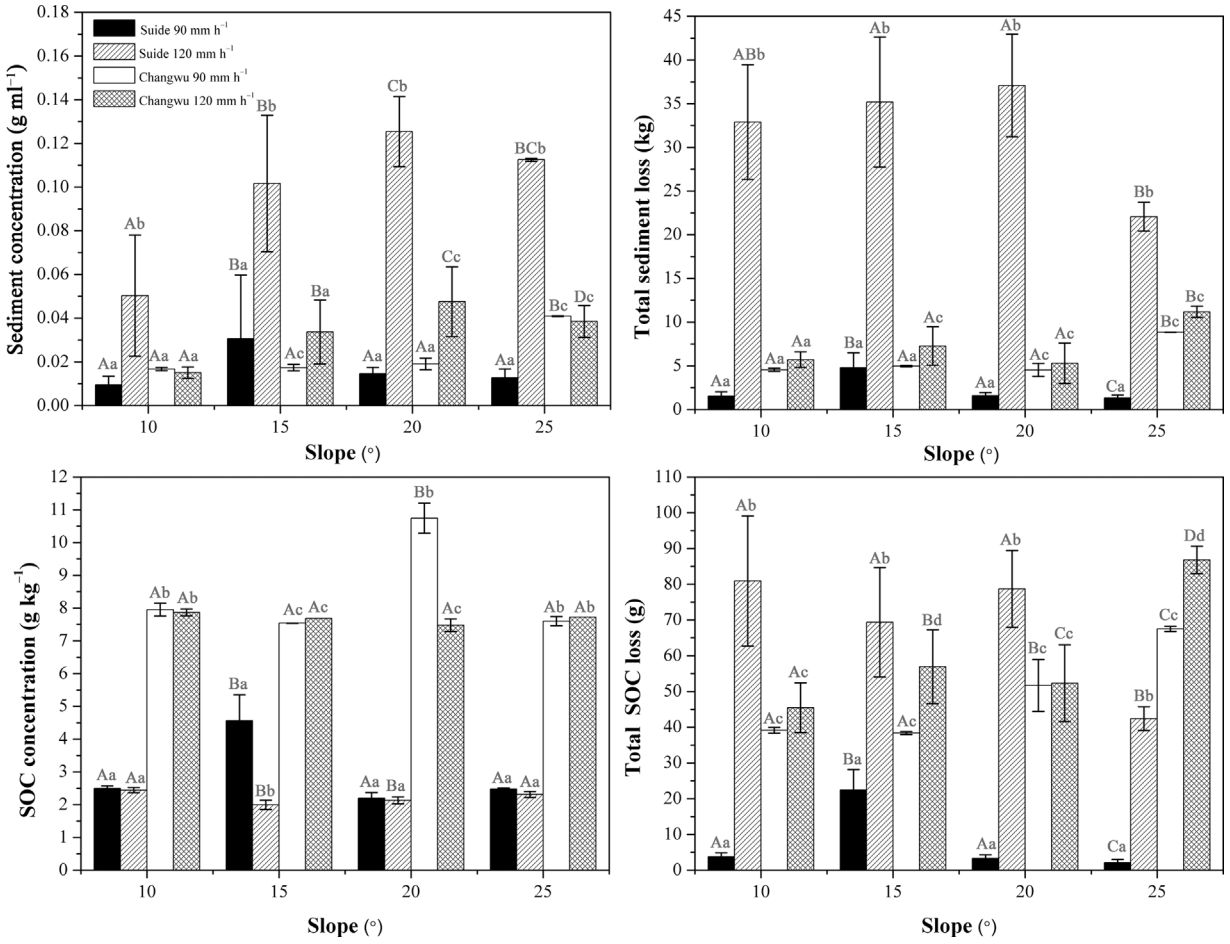

Fig. 1. The sediment concentration, the total sediment loss, the SOC concentration and the total SOC loss distribution for the Suide and Changwu soils with experimental slopes of 10°, 15°, 20° and 25°. Uppercase letters indicate the significant differences between the treatments, with the same slope for the four soils at $P < 0.05$. Lowercase letters indicate the significant differences between the treatments for one soil at $P < 0.05$.

from the outlet. To reduce the experimental error, the flow velocities for each of the two replicated experiments were measured by the same person. After taking the flow velocity measurements at the first location, the flow velocity at each of the remaining three locations was measured in succession. Once the flow velocity was measured at the last location, the flow velocity at the first location was measured again. In addition, after the initiation of rill erosion, the flow velocity was measured at the location where the rill erosion occurs.

2.4. Sample collection and measurement

For each rainfall event, the runoff volume was instantly recorded during the experimental process. After letting the collected runoff samples sit, the sediments were separated from the water, dried and weighed in forced-air ovens at 60 °C for 24 h. Total sediment loss was defined as the total sediment load present in the runoff water. Because the internal flow velocity and surface flow velocity were different, the experimental velocity measurements obtained the maximum surface flow velocities, which were multiplied by a correction factor, α, to obtain the exact flow velocity (Zhang et al., 2010). According to previous studies, for different soils, the value of α ranges between 0.2 and 0.8. The correction factor increased with the velocity or Reynolds number for laminar flow, and could be as high as 0.83 for turbulent flow (Planchon et al., 2005). According to Zhang et al. (2010), the correction factor α of sediment-laden flow varied from 0.233 to 0.682, with a mean value of 0.466. Therefore, 0.466 and 0.8 were selected as the correction factors for interrill flow and rill flow, respectively, which is consistent with Wang and Shi (2015). Before and after the dispersion treatment, the sediment particle distribution of each sample was analyzed twice using a Malvern Mastersizer 2000 laser diffraction device (Malvern Instruments Ltd., UK). To disperse the soil particles, the samples were treated with H_2O_2 to remove any organic matter and with sodium hexametaphosphate for chemical dispersion, before being subjected to ultrasonic dispersion. The other basic properties of the soil were determined by traditional methods (Liu et al., 1996). The SOC concentration of each sample was determined by the dichromate oxidation method (Walkley and Black, 1934) and was defined as the SOC load per kilogram of sampled sediments. SOC loss was defined as the total SOC load present in the total sediment loss.

2.5. Data analysis

All statistical analyses were conducted with either SPSS 19.0 or Origin 8. Pearson correlation analyses were used to study the correlations of the flow velocity, flow depth, hydraulic parameters (stream power and shear stress), sediment loss and SOC loss. The flow velocity, flow depth and hydraulic parameters for each treatment were calculated as the average values for the entire experimental erosion process. One-way analysis of variance (Duncan's test at a = 0.05) was conducted to compare the hydraulic variables, sediment losses and SOC losses of each treatment. Linear regression analysis was conducted to investigate the relationship of the flow velocity with the SOC concentration in the sediments. Nonlinear regression analysis was used to investigate the relationship of the total sediment loss with the SOC enrichment ratio. The flow depth, shear stress and stream power were determined as follows (Mahmoodabadi et al., 2014; Nearing et al.,

Table 2
Results of the soil erosion and SOC loss for the soils from Suide and Changwu.

Soil type	Rainfall intensity (mm h^{-1})	Slope (°)	Time to runoff initiation (min)	Time to rill initiation (min)	Sediment concentration (kg L^{-1})	Total sediment loss (kg)	SOC concentration (g kg^{-1})	*ERoc*	Total SOC loss (kg)
Suide	90	10	5.24	none	0.010	1.92	2.49	1.21	0.004
		15	7.29	26	0.030	7.15	4.56	2.22	0.022
		20	6.30	none	0.014	2.42	2.20	1.07	0.003
		25	7.50	none	0.013	1.82	2.48	1.20	0.002
	120	10	3.50	20	0.050	20.50	2.44	1.19	0.080
		15	3.2	18	0.101	37.18	2.00	0.97	0.069
		20	4.06	18	0.125	39.18	2.13	1.03	0.079
		25	4.45	24	0.112	26.34	2.31	1.12	0.042
Changwu	90	10	2.30	none	0.017	5.78	7.95	1.25	0.039
		15	2.43	none	0.017	6.12	7.54	1.19	0.038
		20	2.12	none	0.019	5.57	10.75	1.69	0.052
		25	2.51	30	0.040	13.35	7.60	1.19	0.067
	120	10	2.06	40	0.015	6.147	7.87	1.24	0.045
		15	2.01	39	0.034	13.66	7.68	1.21	0.057
		20	1.32	18	0.048	17.69	7.48	1.18	0.040
		25	2	26	0.039	13.60	7.72	1.21	0.087

ERoc: the enrichment ratio of soil organic carbon.

1997):

$$D = \frac{q}{V} \quad (1)$$

$$\tau = \rho g D S \quad (2)$$

$$\omega = \rho g S q \quad (3)$$

where D is the average flow depth (m), q is the average unit flow discharge per unit width ($m^2\ s^{-1}$), V is the measured flow velocity ($m\ s^{-1}$), τ is the shear stress (Pa), ρ is the density of water (assumed to have a constant value of 1000 kg m^{-3} at 25 °C), g is the gravitational constant (9.8 $m\ s^{-2}$), S is the slope gradient ($m\ m^{-1}$) and ω is the stream power ($W\ m^{-2}$).

3. Results

3.1. Sediment loss and SOC loss

At the rainfall intensity of 120 mm h^{-1}, the silt loam soil suffered from serious rill soil erosion, and a large amount of sediment was eroded from the slope (Fig. 1 and Table 2). Due to the considerable sediment loss, the amount of SOC loss from the silt loam soil was also large. Therefore, rainfall intensity has a greater effect than slope on sediment and SOC loss from silt loam soils. Furthermore, under both rainfall intensities (90 mm h^{-1} and 120 mm h^{-1}), the sediment concentration and sediment loss of the silt loam soil were consistently greatest at slopes of 15° and 20°, respectively (Fig. 2). For the silty clay soil, the sediment loss and SOC loss did not consistently show significant differences under the different rainfall intensities; thus, slope clearly has a greater effect than rainfall intensity on sediment and SOC losses. For the silty clay soil, the sediment concentration, sediment loss and SOC loss all increased with the slope angle. Additionally, the SOC enrichment ratio of the silt loam was larger than that of the silty clay soil, which was between 0.97 and 2.22 for the former and between 1.18 and 1.69 for the latter (Table 2). For both soils, under 90 mm h^{-1} rainfall, two treatments resulted in significant, large SOC enrichment ratios. One is the treatment with a slope of 15° for the silt loam soil, and the other is the treatment with a slope of 20° for the silty clay soil. Under 120 mm h^{-1} rainfall, the SOC concentrations for both soils did not show significant differences.

3.2. The relationships of hydraulic factors and sediment losses

In our study, under the rainfall intensities of 90 mm h^{-1} and 120 mm h^{-1}, the average flow velocity was greatest for slopes of 15° and 20°, respectively, which is consistent with the sediment concentrations and total sediment losses of the silt loam soil; however, those of the silty clay soil did not present the same obvious regulation (Figs. 1 and 2). Although the runoff depth decreased with slope, it did not show the same trend as the other sediment parameters calculated for the two soils. However, for the rainfall intensity of 120 mm h^{-1}, the stream power showed the same trend as the sediment concentrations and sediment losses for the silt loam soil, but this trend was not observed for the rainfall intensity of 90 mm h^{-1}. Additionally, the shear stress of the silt loam soil did not show an obvious relationship with the slope. However, for the silty clay soil, the stream power and shear stress increased with the slope angle, as did the sediment concentrations and sediment losses. Therefore, the average flow velocity and runoff depth changed proportionally with the slope for the silt loam soil but did not do so with the other hydraulic variables, whereas the stream power changed proportionally with the slope for the silty clay soil but did not do so with the other hydraulic characteristics. Overall, the flow velocity directly affected on sediment loss for the silt loam soil, whereas the stream power directly affected the sediment loss for the silty clay soil. Additionally, all the sediment loss parameters increased with increased rainfall intensity.

3.3. The relationships of hydraulics factors and SOC losses

Considering the combined effects of the soil type and slope, for the rainfall intensity of 90 mm h^{-1}, the average flow velocities significantly affected the total sediment loss ($P < 0.05$), the SOC concentration and the total SOC loss ($P < 0.01$) (Table 3). The stream power was significantly correlated with the sediment concentration and total sediment loss ($P < 0.05$). For the rainfall intensity of 120 mm h^{-1}, the runoff depth was negatively correlated with the sediment concentration and positively correlated with the SOC concentration ($P < 0.01$) (Table 4). According to the linear regression method, the average flow velocity for each treatment was significantly and linearly correlated with the SOC concentration ($R^2 = 0.731$ and $P < 0.001$), especially under the rainfall intensity of 90 mm h^{-1} ($R^2 = 0.958$ and $P < 0.001$) (Fig. 3). Because the flow velocities were consistently high for the soils with large clay percentages and SOC concentrations, we concluded that the clay percentage or SOC contents were positively correlated to the flow velocities for these loess soils. However, under the rainfall intensity of 90 mm h^{-1}, the flow velocities were not only controlled by soil properties but also positively correlated with the SOC concentrations in the sediments. Under the rainfall

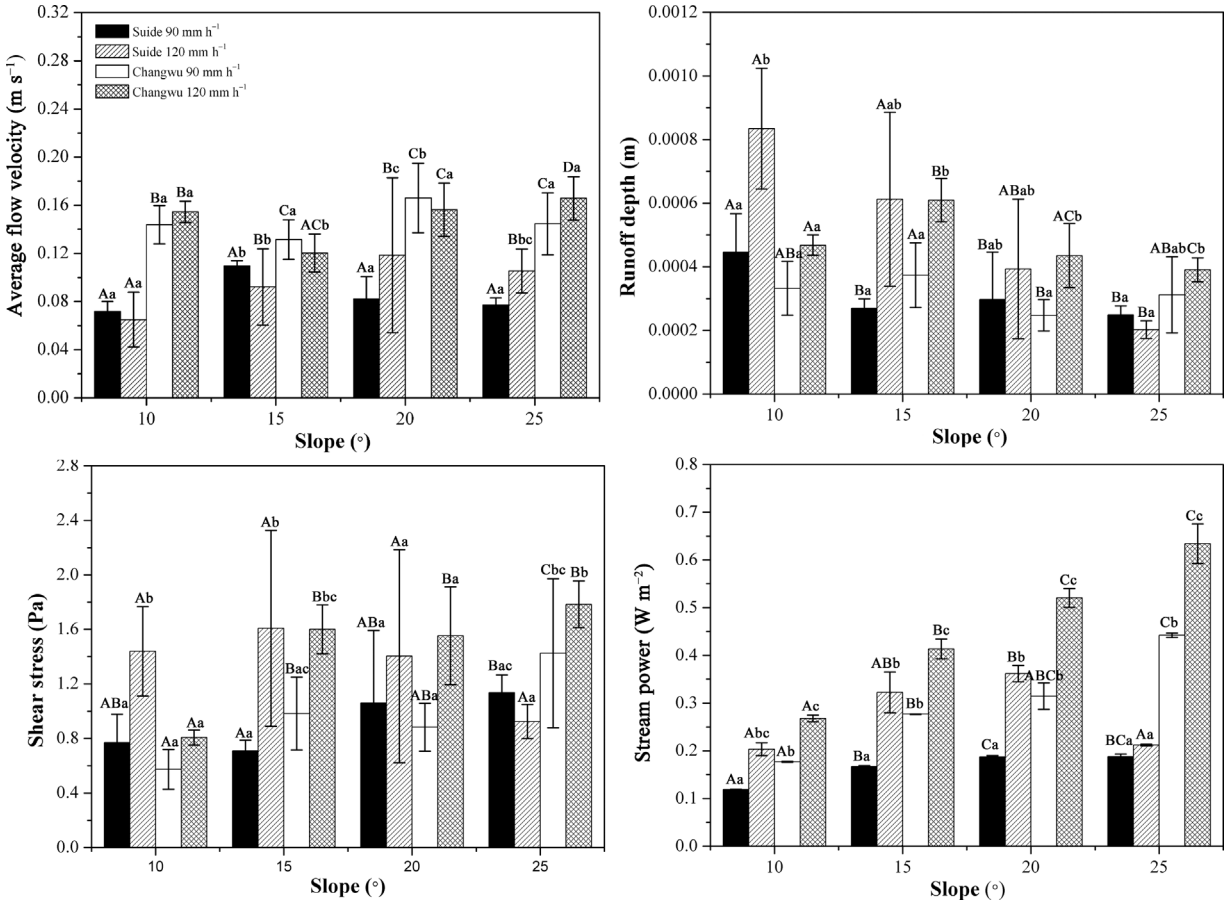

Fig. 2. The hydraulic parameter distribution for the Suide and Changwu soils with different slopes (10°, 15°, 20° and 25°). Uppercase letters indicate the significant differences between the treatments, with the same slope for the four soils at $P < 0.05$. Lowercase letters indicate the significant differences between the treatments for one soil at $P < 0.05$.

intensity of 120 mm h^{-1}, the SOC enrichment ratio displays a significant positive exponential relationship with the total sediment loss (Fig. 4).

3.4. Selective transport of the sediment particles affected by the hydraulic factors

For all treatments, during the first 20 min of rainfall, the clay percentages in the sediments quickly increased with time, whereas the percentages of sand particles clearly decreased (Fig. 5). Therefore, the large light aggregates were consistently transported first by overland flow during the early stages of rainfall. However, over the entire erosion process, clay percentages in the sediments under 90 mm h^{-1} rainfall were consistently higher than those under 120 mm h^{-1} rainfall. Thus, clay particles were easily enriched in the loess soils. In fact, the original silt loam soil with 32.1% coarse sand particles usually generated runoff sediments with > 32% coarse sand particles. The original silty clay soil with 9.5% coarse sand particles generated runoff sediment containing > 15% coarse particles (Table 1 and Fig. 6). Therefore, the aggregates and sand particles were prone to transport under either rainfall intensity tested, even if the clay particles were also enriched during the sheet/interrill erosion. Except for the treatment with a 15° slope and 90 mm h^{-1} rainfall, the effective/ultimate particle size distribution ratios in the coarse silt and sand fractions were above 1.0 and

Table 3
Correlation coefficients of the hydraulic parameters versus the sediment and SOC losses for the Suide and Changwu soils under 90 mm h^{-1} rainfall.

Parameters	Average flow velocity (m s^{-1})	Depth (m)	Shear stress (Pa)	Stream power (W m^{-2})	Sediment concentration (kg L^{-1})	Total sediment loss (kg)	SOC concentration (g kg^{-1})	Total SOC loss (kg)
Average flow velocity (m s^{-1})	1							
Depth (m)	−0.258	1						
Shear stress (Pa)	−0.020	−0.223	1					
Stream power (W m^{-2})	0.682	−0.256	0.703	1				
Sediment concentration (kg L^{-1})	0.639	−0.313	0.413	0.793*	1			
Total sediment loss (kg)	0.765*	−0.103	0.331	0.824*	0.945**	1		
SOC concentration (g kg^{-1})	0.982**	−0.181	−0.057	0.642	0.520	0.679	1	
Total SOC loss (kg)	0.928**	−0.145	0.246	0.855**	0.817*	0.927**	0.891**	1

* Correlation is significant at the 0.05 level (two-tailed).
** Correlation is significant at the 0.01 level (two-tailed).

Table 4
Correlation coefficients of the hydraulic parameters versus the sediment and SOC losses for the Suide and Changwu soils under 120 mm h^{-1} rainfall.

Parameters	Average flow velocity (m s^{-1})	Depth (m)	Shear stress (Pa)	Stream power (W m^{-2})	Sediment concentration (kg L^{-1})	Total sediment loss (kg)	SOC concentration (g kg^{-1})	Total SOC loss (kg)
Average flow velocity (m s^{-1})	1							
Depth (m)	0.224	1						
Shear stress (Pa)	0.473	0.304	1					
Stream power (W m^{-2})	0.919**	0.436	0.691	1				
Sediment concentration (kg L^{-1})	−0.416	−0.912**	−0.105	−0.519	1			
Total sediment loss (kg)	−0.508	−0.714	0.089	−0.475	0.928**	1		
SOC concentration (g kg^{-1})	0.544	0.838**	0.116	0.622	−0.973**	−0.944**	1	
Total SOC loss (kg)	0.085	−0.056	0.694	0.336	0.282	0.500	−0.236	1

*Correlation is significant at the 0.05 level (two-tailed).
**Correlation is significant at the 0.01 level (two-tailed).

near 1.0, respectively. Under 120 mm h^{-1} rainfall, the effective/ultimate ratios of coarse silt particles were all less than 1.0 whereas the effective/ultimate ratios of sand particles were all above 1.0. These results indicated that for the silt loam soil clay-bonded microaggregates (0.02–0.05 mm) were prone to transport under 90 mm h^{-1} rainfall, whereas large macroaggregates were easily transported under 120 mm h^{-1} rainfall. For the silty clay soil, although the percentages of each particle size in the sediments varied considerably under 90 mm h^{-1} rainfall, there is not a clear difference between the two rainfall intensities.

For the silt loam soil, the sediment loss of the treatment with a slope of 15° under 90 mm h^{-1} rainfall was significantly less than those under 120 mm h^{-1} rainfall, and the median diameters of the effective sediment particles decreased (Fig. 1 and Table 5). Thus, although rill erosion occurred with this treatment, interrill erosion still played an important role. Additionally, the median diameter of the effective sediment particles of the treatment with a slope of 15° was significantly larger than the other treatments under 90 mm h^{-1} rainfall. The clay percentage in sediments and the effective/ultimate ratios of clay particles for the treatment with a slope of 15° were the lowest under 90 mm h^{-1} rainfall (Figs. 5 and 6). Therefore, under 90 mm h^{-1} rainfall, high flow velocities induced by rill erosion resulted in large amounts of clay-bonded aggregates first transported from the silt loam soil. For the silty clay soil under 90 mm h^{-1} rainfall, both the percentages of the clay particles in the sediments and the flow velocities have the highest values for the treatment with a slope of 20°. Under 90 mm h^{-1} rainfall, the median diameter of the effective sediment particles of the treatment with a slope of 20° was the lowest, while the median diameter of the ultimate sediment particles of this treatment was the largest. Hence, the clay particles were clearly enriched in the sediments generated from this treatment. Overall, under 90 mm h^{-1} rainfall, flow velocities are closely related with the transport of light particles (light aggregates or clay particles), but this was not true for other hydraulic variables (e.g., runoff depth, shear stress and stream power). Under the rainfall intensity of 120 mm h^{-1}, the flow velocity did not have a clear relationship with the transport of sediment particles.

3.5. Processes of SOC loss affected by hydraulic factors

According to the time variations of the SOC enrichment ratio for each treatment in both the silt loam and silty clay soils (Fig. 8), the SOC enrichment ratio was consistently large at the beginning of the soil erosion process, and then decreased during the experiment, becoming stable within 10 min. For the silt loam soil, under the rainfall intensity of 90 mm h^{-1}, only the treatment with a slope of 15° had a clear SOC enrichment ratio trend during the whole erosion process. Under the rainfall intensity of 120 mm h^{-1}, the SOC enrichment ratio for the silt loam soil remained approximately 1.0 throughout the erosion process. For the silty clay soil, the treatment with a slope of 20° and rainfall intensity of 90 mm h^{-1} was the only treatment in which a large SOC enrichment ratiowas observed. However, the SOC enrichment ratio for the silty clay soil was consistently slightly greater than 1.0 under the rainfall intensity of 120 mm h^{-1}. Additionally, for the silt loam soil under the rainfall intensity of 90 mm h^{-1}, the flow velocity of the treatment that accompanied the large SOC concentration was also

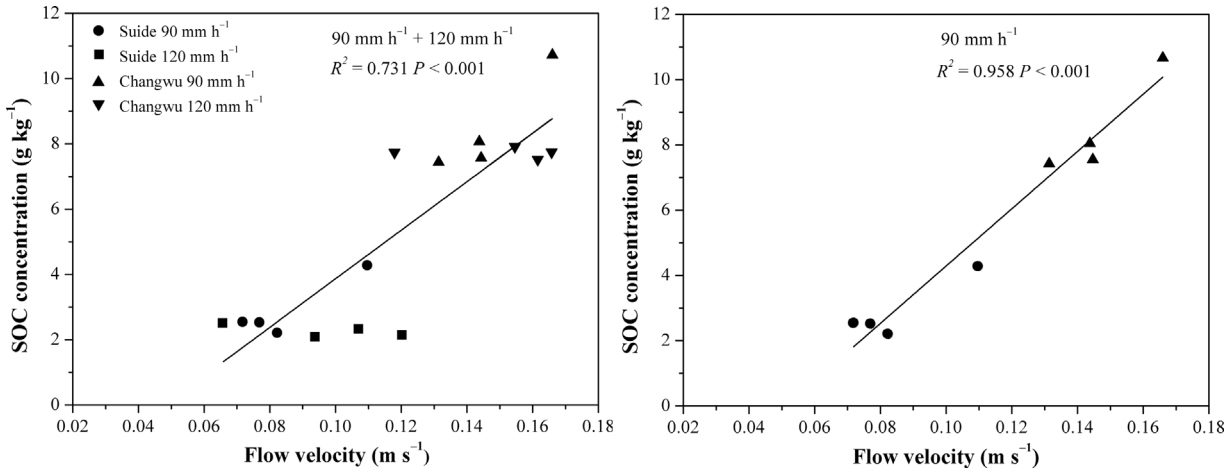

Fig. 3. The linear relationship between the average flow velocities and the SOC concentration for the rainfall intensities of 90 mm h^{-1} and 120 mm h^{-1} (note that the (b) was only for the rainfall intensity of 90 mm h^{-1}).

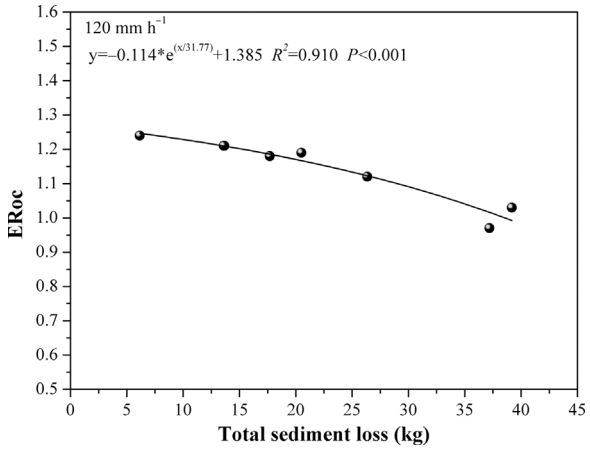

Fig. 4. Exponential relationship between the total sediment loss and SOC enrichment under a rainfall intensity of 120 mm h^{-1}.

consistently significantly higher than the other treatments throughout the whole rainfall process (Fig. 7). For the silty clay soil, the flow velocity of the treatment that accompanied a large SOC concentration fluctuated considerably and also had the highest velocity.

For the silt loam soil, during the erosion process, of the treatment with a slope of 15° and a large SOC enrichment ratio, the clay particles were clearly less common than those of all the other treatments under 90 mm h^{-1} rainfall (Fig. 5). The percentage of sand particles in the sediments was obviously higher than those of all the other treatments. Therefore, the silt, clay, and light aggregates, which contain large organic carbon loads in the silt loam soil, were transported first, resulting in a large SOC enrichment ratio of 90 mm h^{-1}. However, for the silty clay soil, the percentage of clay particles in the sediments of the treatment with a large SOC enrichment ratio was larger than that observed in all other treatments. The percentages of sand in the sediments of the treatment with a slope of 20° under the 90 mm h^{-1} rainfall intensity were lower than those in the other treatments. Additionally, the effective/ultimate ratios of the clay particles for the above scenario were closer to 1.0 than all the other treatments under 90 mm h^{-1} rainfall. These observations indicate that the SOC was mainly bonded with clay particles for the silty clay soil and was enriched in the sediments under 90 mm h^{-1} rainfall, which lead to increased SOC concentrations. Therefore, the soil texture has an important effect on the mechanisms of sediment particle transport and SOC loss because it affects the hydraulic factors (e.g. flow velocity).

4. Discussions

4.1. Mechanisms for the selective transport of sediment particles

Moss et al. (1979) noted that suspended, saltating and contact (rolling) loads were normally broadly associated with particular sediment size ranges. Clay and silt particles in loess soils were mainly associated with suspension-saltation transport, while the coarse fractions were mainly transported by rolling (Shi et al., 2012). In our study, when

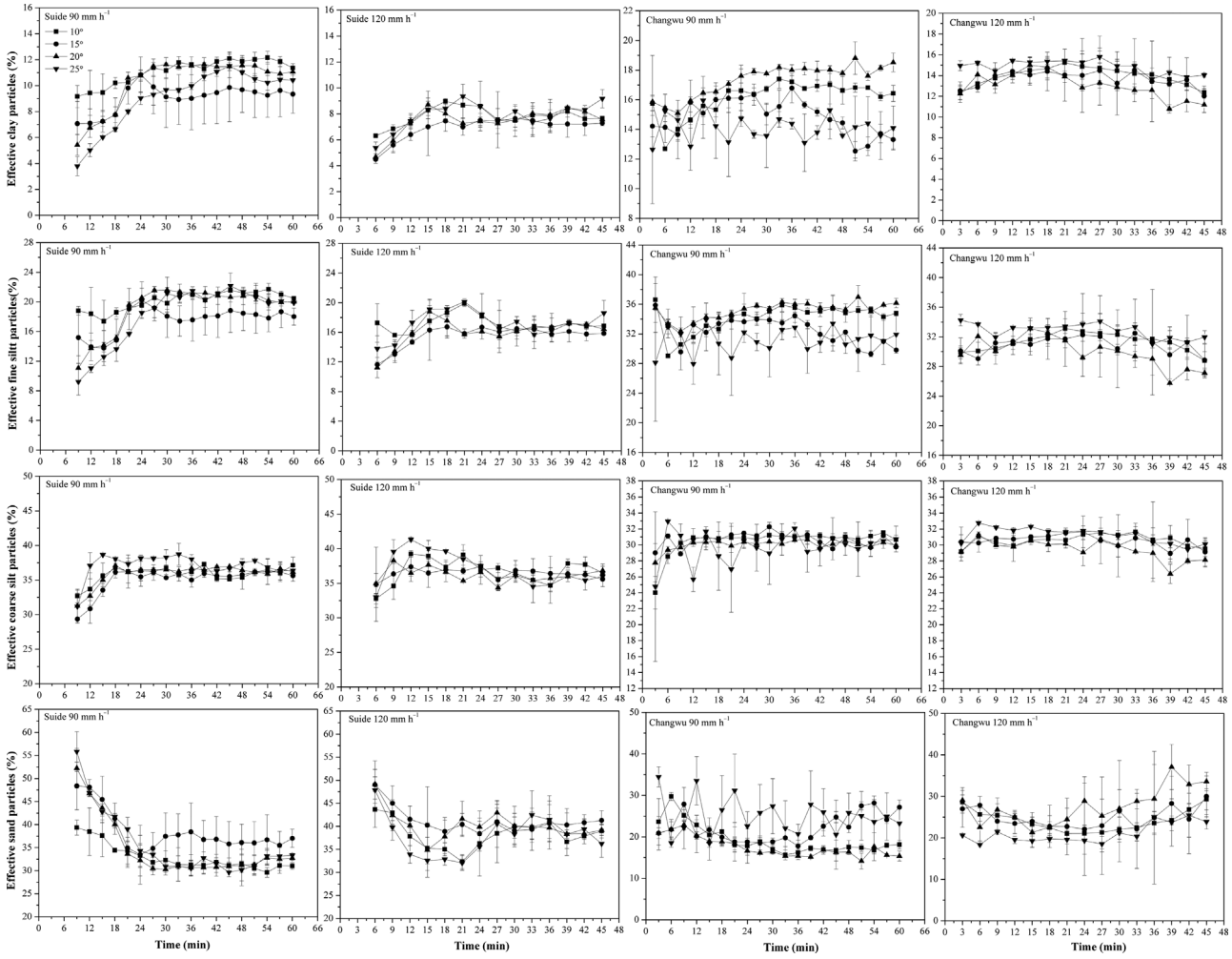

Fig. 5. Temporal variations in the percentages of the effective sediment particles on the four selected slopes for the two soils from Changwu (CW) and Suide (SD).

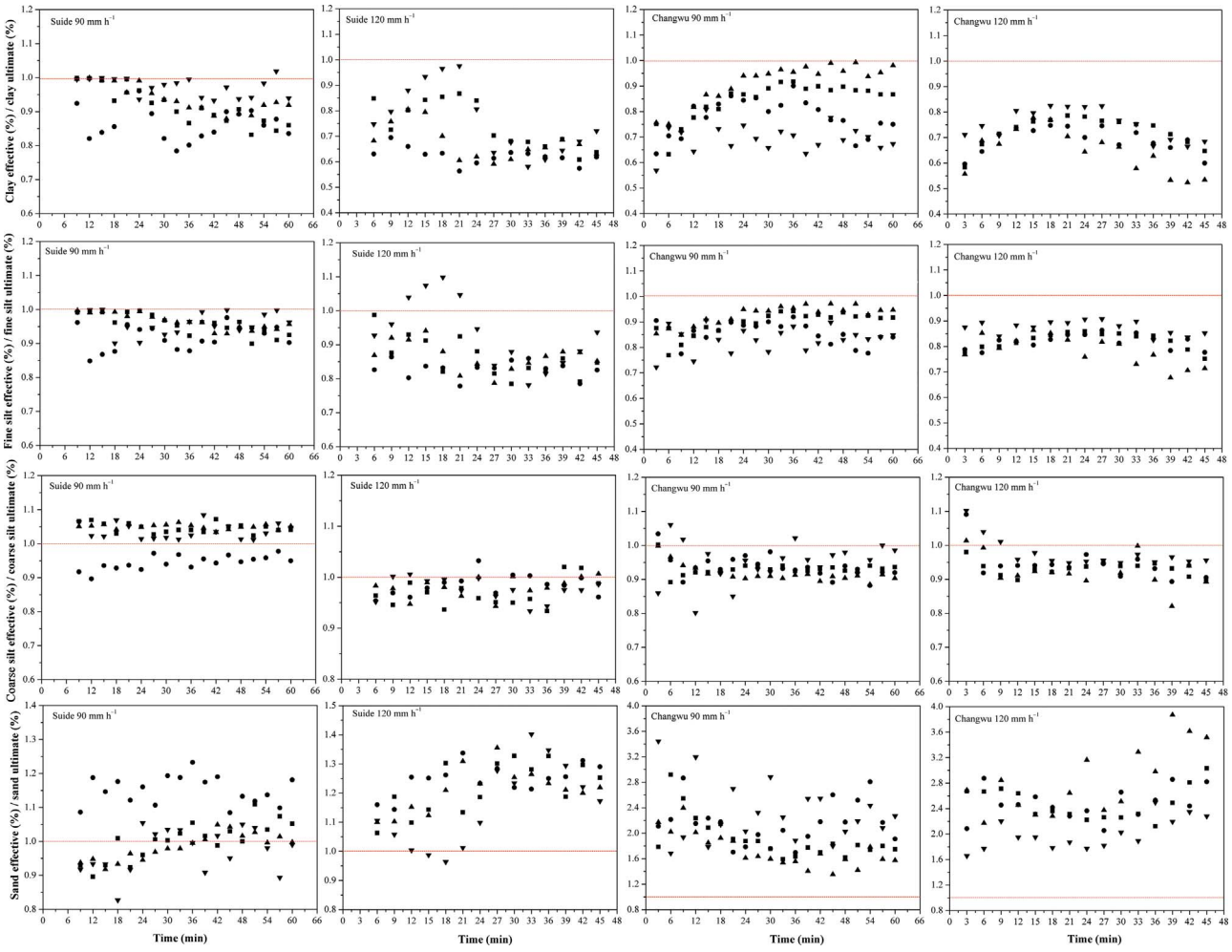

Fig. 6. Comparison of the effective/ultimate particle size distribution ratios in the clay, fine silt, coarse silt, and sand fractions of the Changwu (CW) and Suide (SD) soils on the four selected slopes.

Table 5
Median diameter (μm) of the effective and ultimate sediment particles from the Suide (SD) and Changwu (CW) soils with different slopes and rainfall intensities.

Slope	SD		CW	
	90 mm h^{-1}	120 mm h^{-1}	90 mm h^{-1}	120 mm h^{-1}
Effective				
10	38.93a	43.81a	21.46a	25.04ab
15	43.54b	46.54b	23.55b	27.60a
20	40.11a	45.62b	19.89c	22.35b
25	40.80a	43.61a	25.79d	23.13b
Ultimate				
10	38.20a	37.83a	17.40a	17.30a
15	39.48b	39.06b	17.94b	17.11a
20	40.13b	39.39b	17.40a	17.28a
25	41.41c	39.34b	16.87c	17.13a

Values for the effective/ultimate sediment particles in a column followed by the same letter are not significantly different at $P < 0.05$.

only sheet and splash erosion occurs, the flow velocities are closely related to the transport of clay or large light aggregates. Both soil type and hydraulic flow characteristics determine the transport mechanisms (Asadi et al., 2011). Hence, the flow velocity is associated with suspension-saltation transport for the silty clay and rolling transport for the silt loam; these associations also need to be further investigated. We observed that the stream powers, also associated with rolling load (Shi et al., 2012), of the silt loam soil were consistently lower than those of the silty clay soil potentially because the rolling of large sediment particles could consume more energy in the coarse-textured soil (Fig. 2). After rill development or on steep hillslopes, bed-load transport by rolling of large particles becomes an important transport mechanism that increases the coarse-sand-sized particle content after rill initiation (Asadi et al., 2007). In addition, the sediments from the loess soils contain more coarse particles than the original soils because the clay and silt particles were more likely transported as aggregates to the loess soils, which is consistent with the observations of Wang and Shi (2015). Overall, hydraulic flow characteristics and soil type have important effects on sediment size distribution and sediment transport (Loch and Donnollan, 1983; Shi et al., 2012).

4.2. Mechanisms of the hydraulic parameters controlling SOC concentrations

With lower rainfall intensity, the flow velocity had a significant positive effect on the SOC concentration because it controlled the preferential transport of the light SOC-enriched sediment fraction. For the coarse-textured soil with a lower clay percentage and SOC content, the initial transport of the light aggregates was responsible for the SOC enrichment, but the selective transport of the fine particles resulted in the SOC enrichment of the fine-textured soils with large SOC contents. In general, this selective process has been attributed to the selective transport of fine particles or the depletion of heavy particles (Maïga-Yaleu et al., 2015; Martínez-Mena et al., 2012; Polyakov and Lal, 2004a). In our study, although parts of the clay particles were included

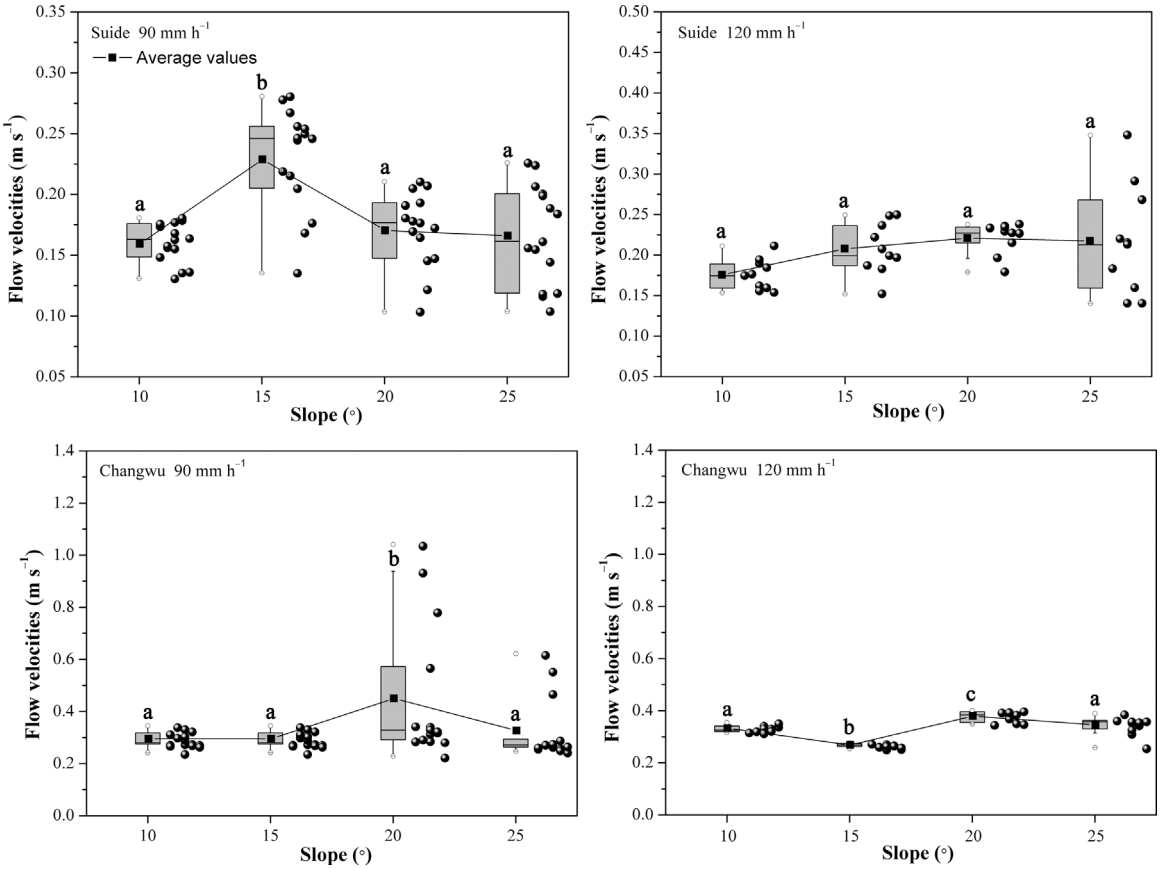

Fig. 7. Comparisons of the flow velocities for the Suide and Changwu soils on different slopes (10°, 15°, 20° and 25°) and for different rainfall intensities (90 and 120 mm h^{-1}). The different letters indicate significant differences at $P < 0.05$.

in the aggregates of the loess soils (Wang and Shi, 2015), soils with different textures underwent the selective transport of different particles, which contributed to the SOC enrichment. Specifically, for the loess soils, the clay percentage and SOC content of the original soils had a considerable effect on the flow velocities. The flow velocity associated with the suspension-saltation or rolling of the sediments was a good descriptor of the SOC enrichment in sediments, especially when only interrill erosion occurred. If the SOC is mainly concentrated in the heavy aggregates, it becomes difficult for the soil to enrich in SOC, and the SOC concentrations are not related to the flow velocity. In fact, the SOC within large low-density aggregates displays higher mineralization ratios than those within particles less than 0.050 mm in size (Martínez-Mena et al., 2012). This difference occurs because the soil aggregates are broken up during the soil erosion process (Shi et al., 2010), and the loss of the SOC in the aggregates promotes microbial mineralization (Starr et al., 2000). Additionally, the mineral-associated organic carbon stabilizes with the silt and clay particles and is critical to the persistence of SOC (Cai et al., 2016; Nie et al., 2017; Polyakov and Lal, 2008; Trigalet et al., 2014). Therefore, the coarse-textured loess soil contributes more than the fine-textured soils to SOC loss to the atmosphere. Finally, the relationships of the hydraulic characteristics and SOC concentration should be used in SOC loss prediction. However, the relationships of the hydraulic variables and the transport of sediment and SOC in other soils need to be further investigated.

Under high rainfall intensity, the silty clay soil consistently had a slightly higher SOC enrichment ratio than the silt loam soil because of the high clay content and SOC content in the silty clay soil. Additionally, runoff depth showed clear, direct relationships with the SOC concentrations under high rainfall intensity. Runoff depth, which may also be correlated with the sediment transport mechanism, was a good descriptor of the SOC concentration under the high rainfall intensity, which will be further investigated in future studies. In previous studies, the enrichment ratio of OC decreased with increasing soil loss (Fiener et al., 2015; Polyakov and Lal, 2004a) and consistently had a significant power relationship with the total sediment loss after rainfall (Li et al., 2015). In our study, the enrichment ratio of the OC had a significant exponential relationship with the total sediment loss under only the high rainfall intensity. This result was observed because at the initiation of the runoff, the fine particles or light SOC-enriched fraction was transported, and the rill erosion later decreased the SOC enrichment ratio (Fiener et al., 2015; Polyako and Lal, 2004a; Schiettecatte et al., 2008a). Studying the dynamic flow velocity mechanism affecting the SOC concentrations will provide important knowledge about the SOC loss process and will help to regulate SOC transport.

4.3. The relationships of hydraulic factors with sediment and SOC losses

Flow depth, flow velocity and hydraulic parameters (e.g., shear stress, stream power, and unit stream power) are usually used to characterize the erosive powers of overland flows and to determine sediment concentrations (Shih and Yang, 2009; Trout and Neibling 1993). In soil erosion models, e.g., the Water Erosion Prediction Project (WEPP) (Nearing et al., 1989), Limburg Soil Erosion Model (LISEM) (De Roo et al., 1996) and European Soil Erosion Model (EUROSEM) (Morgan et al., 1998), the transport capacity was also generally estimated by hydraulic parameters (Govers, 1990). In our study, under different rainfall intensities, the hydraulic characteristics have different relationships with the sediment and SOC loss parameters. Thus, the rainfall intensity could change the relationships of the hydraulic characteristics with sediment and SOC losses, which should be considered in the estimation of sediment and SOC loss for the loess soils. Under the

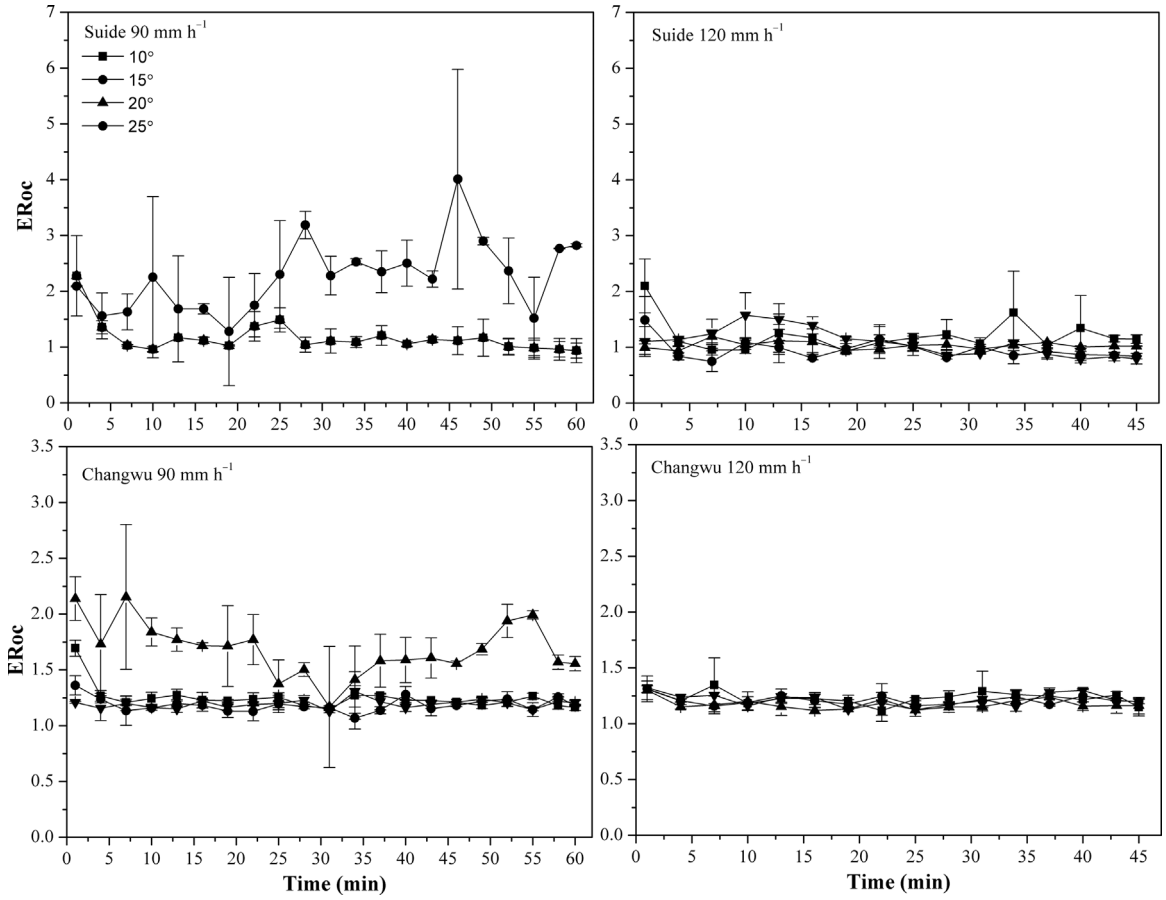

Fig. 8. Time variation of the SOC enrichment ratio (*ERoc*) in the sediments of the Suide and Changwu soils under the rainfall intensities of 90 mm h $^{-1}$ and 120 mm h $^{-1}$ for the different slope of 10°, 15°, 20° and 25°.

low rainfall intensity, stream power, usually used as a measure of the erosive forces associated with the flowing waters for both interrill and rill erosion (Kinnell, 2005; Nearing et al., 1997; Shi et al., 2012), was a good descriptor for sediment loss, while the flow velocity was a good descriptor for SOC concentration. However, under high rainfall intensity, no direct relationships existed between the hydraulic variables and sediment loss because the sediment concentration usually attained the maximum sediment transport capacity when serious rill erosion occurred. Considering the effect of soil texture, the slope had a more important and direct effect on the sediment and SOC loss in the fine-textured soil than in the coarse-textured soil, which is consistent with the results of our previous studies (Li et al., 2016b). Additionally, spatially distributed hydrologic models are often used to predict the excess flows and sediment transport processes in a watershed (Shih and Yang, 2009). Therefore, our researches serve as important references to improve or build a sediment or SOC model. However, the relationships of the hydraulic factors with the sediment and SOC losses on gauging station at small catchment scale should be further investigated in the future.

5. Conclusions

The relationships of hydraulic factors with sediment and SOC losses were investigated for two soils with different textures and a range of slopes. The results suggested that the flow velocity associated with the suspension or rolling transport is positively related to the SOC concentration during the interrill erosion process. However, the runoff depth had a close relationship with the SOC concentration in the high rainfall intensity experiments. Among the four hydraulic variables, stream power was the best descriptor of sediment loss for the interrill erosion. For the coarse-textured soil, the selective transport of light aggregates and large sediment losses could result in more SOC lost to the atmosphere than for the fine-texture soil. In addition, rainfall intensity could change the relationships of the hydraulic factors and sediment and SOC loss by controlling soil erosion process. The slope had a more important and direct effect on the sediment and SOC loss from the fine-textured soil than from the coarse-textured soil. The relationships of the hydraulic factors and the sediment and SOC losses provide important references for building hydraulic-based sediment or SOC models.

Acknowledgments

This study was financially supported by the “Hundred-Talent Project” of the Chinese Academy of Sciences and the National Natural Science Foundation of China (41271294).

References

Agata, N., Artemi, C., Carmelo, D., Giuseppe, L.P., Antonino, S., Luciano, G., 2015. Effectiveness of carbon isotopic signature for estimating soil erosion and deposition rates in Sicilian vineyards. Soil Till. Res. 152, 1–7.

Arjmand, S.S., Mahmoodabadi, M., 2015. Sediment concentration and hydraulic characteristics of rain-induced overland flows in arid land soils. J. Soil Sediments 15 (3), 710–721.

Asadi, H., Ghadiri, H., Rose, C.W., Yu, B., Hussein, J., 2007. An investigation of flow-driven soil erosion processes at low streampowers. J. Hydrol. 342, 134–142. http://dx.doi.org/10.1016/j.jhydrol.2007.05.019.

Asadi, H., Moussavi, A., Ghadiri, H., Rose, C.W., 2011. Flow-driven soil erosion processes and the size selectivity of sediment. J. Hydrol. 406, 73–81.

Cai, A., Feng, W., Zhang, W., Xu, M., 2016. Climate, soil texture, and soil types affect the contributions of fine-fraction-stabilized carbon to total soil organic carbon in different land uses across China. J. Environ. Manag. 172, 2–9.

Comprehensive Scientific Expedition, C.M., 1990. Slope classification data set of cultivated land on Loess Plateau area. Nat. Sci. Technol. Infrastructure China, Data Sharing Infrastructure Earth Syst. Sci., Chinese Acad. Sci. Beijing. http://www.geodata.cn.
De Roo, A.P.J., Wesseling, C.G., Ritsema, C.J., 1996. LISEM: A single-event physically based hydrological and soil erosion model for drainage basins. I: theory, input and output. Hydrol. Processes 10 (8), 1107–1117.
Fiener, P., Dlugoß, V., Van Oost, K., 2015. Erosion-induced carbon redistribution, burial and mineralisation — is the episodic nature of erosion processes important? Catena 133, 282–292.
Fu, B., 1989. Soil erosion and its control in the Loess Plateau of China. Soil Use Manag. 5 (2), 76–82.
Gilley, J.E., Kottwitz, E.R., Simanton, J.R., 1990. Hydraulic characteristics of rills. Trans. ASAE 33 (6), 1900–1906.
Govers, G., 1990. Empirical relationships for the transport capacity of overland flow. IAHS Publ. 189, 45–63.
Gregorich, E.G., Greer, K.J., Anderson, D.W., Liang, B.C., 1998. Carbon distribution and losses: erosion and deposition effects. Soil Till. Res. 47 (3–4), 291–302.
Huang, J., Li, Z., Zhang, P., Liu, J., Cheng, D., Ren, F., Wang, Z., 2017. CO^2 emission pattern of eroded sloping croplands after simulated rainfall in subtropical China. Ecol. Eng. 99, 39–46.
Kinnell, P.I.A., 2005. Raindrop-impact-induced erosion processes and prediction: a review. Hydrol. Processes 19 (14), 2815–2844.
Kuhn, N.J., Armstrong, E.K., 2012. Erosion of organic matter from sandy soils: solving the mass balance. Catena 98, 87–95.
Kuhn, N.J., Hoffmann, T., Schwanghart, W., Dotterweich, M., 2009. Agricultural soil erosion and global carbon cycle: controversy over? Earth Surf. Processes Landform 34 (7), 1033–1038.
Lal, R., Griffin, M., Apt, J., Lave, L., Morgan, G., 2004. Response to comments on managing soil. Carbon Sci. 305 (5690) 1567–1567.
Lal, R., 2005. Soil erosion and carbon dynamics. Soil Till. Res. 81 (2), 137–142.
Leifeld, J., Bassin, S., Fuhrer, J., 2005. Carbon stocks in Swiss agricultural soils predicted by land-use, soil characteristics, and altitude. Agric. Ecosyst. Environ. 105, 255–266.
Li, Z., Lu, Y., Nie, X., Ma, W., Xiao, H., 2015. Simulating study of the loss of soil organic carbon based on the model of sediment transport by slope runoff in the hilly red soil region of central human province. J. Hunan Univ. (Nat. Sci.) 42 (12), 115–124.
Li, Z., Nie, X., Chang, X., Liu, L., Sun, L., 2016a. Characteristics of soil and organic carbon loss induced by water erosion on the loess plateau in China. PLoS One 11 (4), e0154591.
Li, Z., Liu, L., Nie, X., Chang, X., Liu, C., Xiao, H., 2016b. Modeling soil organic carbon loss in relation to flow velocity and slope on the loess plateau of China. Soil Sci. Soc. Am. J. 80 (5), 1341.
Li, Z., Liu, C., Dong, Y., Chang, X., Nie, X., Liu, L., Xiao, H., Lu, Y., Zeng, G., 2017. Response of soil organic carbon and nitrogen stocks to soil erosion and land use types in the Loess hilly–gully region of China. Soil Till. Res. 166, 1–9.
Liu, G.S., Jiang, N.H., Zhang, L.D., 1996. Soil Physical and Chemical Analysis and Description of Soil Profiles. Standards Press of China, Beijing (In Chinese).
Liu, C., Dong, Y., Li, Z., Chang, X., Nie, X., Liu, L., Xiao, H., Bashir, H., 2017a. Tracing the source of sedimentary organic carbon in the Loess Plateau of China: an integrated elemental ratio, stable carbon signatures, and radioactive isotopes approach. J. Environ. Radioact. 167, 201–210.
Liu, C., Li, Z., Dong, Y., Nie, X., Liu, L., Xiao, H., Zeng, G., 2017b. Do land use change and check-dam construction affect a real estimate of soil carbon and nitrogen stocks on the Loess Plateau of China? Ecol. Eng. 101, 220–226.
Loch, R.J., Donnollan, T.E., 1983. Field rainfall simulator studies on two clay soils of the Darling downs, Queensland. II. Aggregate breakdown, sediment properties and soil erodibility. Aust. J. Soil Res. 21, 47–58.
Ma, W., Li, Z., Ding, K., Huang, J., Nie, X., Zeng, G., Wang, S., Liu, G., 2014. Effect of soil erosion on dissolved organic carbon redistribution in subtropical red soil under rainfall simulation. Geomorphology 226, 217–225.
Ma, W., Li, Z., Ding, K., Huang, B., Nie, X., Lu, Y., Xiao, H., 2016. Soil erosion, organic carbon and nitrogen dynamics in planted forests A case study in a hilly catchment of Hunan Province, China. Soil Till. Res. 155, 69–77.
Maïga-Yaleu, S.B., Chivenge, P., Yacouba, H., Guiguemde, I., Karambiri, H., Ribolzi, O., Bary, A., Chaplot, V., 2015. Impact of sheet erosion mechanisms on organic carbon losses from crusted soils in the Sahel. Catena 126, 60–67.
Mahmoodabadi, M., Ghadiri, H., Rose, C., Yu, B., Rafahi, H., Rouhipour, H., 2014. Evaluation of GUEST and WEPP with a new approach for the determination of sediment transport capacity. J. Hydrol. 513, 413–421.
Martínez-Mena, M., López, J., Almagro, M., Albaladejo, J., Castillo, V., Ortiz, R., Boix-Fayos, C., 2012. Organic carbon enrichment in sediments: effects of rainfall characteristics under different land uses in a Mediterranean area. Catena 94, 36–42.
Meersmans, J., De Ridder, F., Canters, F., De Baets, S., Van Molle, M., 2008. A multiple regression approach to assess the spatial distribution of Soil Organic Carbon (SOC) at the regional scale (Flanders, Belgium). Geoderma 143 (1–2), 1–13.
Morgan, R.P.C., Quinton, J.N., Smith, R.E., Govers, G., Poesen, J.W.A., Auerswald, K., Chisci, G., Torri, D., Styczen, M.E., 1998. The European Soil Erosion Model (EUROSEM): a dynamic approach for predicting sediment transport from fields and small catchments. Earth Surf. Processes Landforms 23 (6), 527–544.
Moss, A.J., Walker, P.H., Hutka, J., 1979. Raindrop-stimulated transportation in shallow water flows: an experimental study. Sediments Geol. 22, 165–184.
Nearing, M.A., Foster, G.R., Lane, L.J., Finkner, S.C., 1989. A process-based soil erosion model for USDA-Water Erosion Prediction Project technology. Trans. ASAE 32 (5), 1587–1593.
Nearing, M.A., Norton, L.D., Bulgakov, D.A., Larionov, G.A., West, L.T., Dontsova, K.M., 1997. Hydraulics and erosion in eroding rills. Water Resour. Res. 33 (4), 865–876.
Nie, X., Li, Z., Huang, J., Huang, B., Xiao, H., Zeng, G., 2017. Soil organic carbon fractions and stocks respond to restoration measures in degraded lands by water erosion. Environ. Manag. 59 (5), 816–825.
Palis, R.G., Ghandiri, H., Rose, C.W., Saffigna, P.G., 1997. Soil erosion and nutrient loss. III. Changes in the enrichment ratio of total nitrogen and organic carbon under rainfall detachment and entrainment. Aust. J. Soil Res. 35 (4), 891–905.
Pan, C., Shangguan, Z., 2006. Runoff hydraulic characteristics and sediment generation in sloped grassplots under simulated rainfall conditions. J. Hydol. 331 (1–2), 178–185.
Parton, W.J., Schimel, D.S., Cole, C.V., Oiima, D.S., 1987. Analysis of factors controlling soil organic matter levels in great plains grasslands. Soil Sci. Soc. Am. J. 51, 1173–1179.
Parton, W.J., Scurlock, J.M.O., Ojima, D.S., Gilmanov, T.G., Scholes, R.J., Schimel, D.S., Kirchner, T., Menaut, J.C., Seastedt, T., Garcia Moya, E., Kamnalrut, A., Kinyamario, J.I., 1993. Observations and modeling of biomass and soil organic matter dynamics for the grassland biome worldwide. Glob. Biogeochem. Cycles 7 (4), 785–809.
Planchon, O., Silvera, N., Gimenez, R., Favis-Mortlock, D., Wainwright, J., Bissonnais, Y.L., Govers, G., 2005. An automated salt-tracing gauge for flow-velocity measurement. Earth Surf. Processes Landforms 30 (7), 833–844.
Polyakov, V.O., Lal, R., 2004a. Modeling soil organic matter dynamics as affected by soil water erosion. Environ. Int. 30 (4), 547–556.
Polyakov, V.O., Lal, R., 2004b. Soil erosion and carbon dynamics under simulated rainfall. Soil Sci. 169 (8), 590–599.
Polyakov, V.O., Lal, R., 2008. Soil organic matter and CO_2 emission as affected by water erosion on field runoff plots. Geoderma 143 (1–2), 216–222.
Rodriguez, A., Guerrra, J.A., Gorrin, S.P., Arbelo, C.D., Mora, J.L., 2002. Aggregates stability and water in andosols of the canary islands. Land Degrad. Dev. 13, 515–523.
Schiettecatte, W., Gabriels, D., Cornelis, W.M., Hofman, G., 2008a. Enrichment of organic carbon in sediment transport by interrill and rill erosion processes. Soil Sci. Soc. Am. J. 72 (1), 50.
Schiettecatte, W., Verbist, K., Gabriels, D., 2008b. Assessment of detachment and sediment transport capacity of runoff by field experiments on a silt loam soil. Earth Surf. Processes Landforms 33 (8), 1302–1314.
Shen, H., Zheng, F., Wen, L., Lu, J., Jiang, Y., 2015. An experimental study of rill erosion and morphology. Geomorphology 231, 193–201.
Shen, H., Zheng, F., Wen, L., Han, Y., Hu, W., 2016. Impacts of rainfall intensity and slope gradient on rill erosion processes at loessial hillslope. Soil Till. Res. 155, 429–436.
Shi, Z.H., Yan, F.L., Li, L., Li, Z.X., Cai, C.F., 2010. Interrill erosion from disturbed and undisturbed samples in relation to topsoil aggregate stability in red soils from subtropical China. Catena 81 (3), 240–248.
Shi, Z.H., Fang, N.F., Wu, F.Z., Wang, L., Yue, B.J., Wu, G.L., 2012. Soil erosion processes and sediment sorting associated with transport mechanisms on steep slopes. J. Hydol. 454–455, 123–130.
Shih, H.M., Yang, C.T., 2009. Estimating overland flow erosion capacity using unit stream power. Int. J. Sediments Res. 24 (1), 46–62.
Slattery, M.C., Bryan, R.B., 1992. Hydraulic conditions for rill incision under simulated rainfall: a laboratory experiment. Earth Surf. Processes Landforms 17 (2), 127–146.
Starr, G.C., Lal, R., Malone, R., Hothem, D., Owens, L., Kimble, J., 2000. Modeling soil carbon transported by water eroion processes. Land Degrad. Dev. 11, 83–91.
Trigalet, S., Van Oost, K., Roisin, C., van Wesemael, B., 2014. Carbon associated with clay and fine silt as an indicator for SOC decadal evolution under different residue management practices. Agric. Ecosyst. Environ. 196, 1–9.
Trout, T.J., Neibling, W.H., 1993. Erosion and sedimentation processes on irrigated fields. J. Irrig. Drain. Eng. 119 (6), 947–963.
Walkley, A., Black, I.A., 1934. An examination of the Degtjareff method for determining soil organic matter, and a proposed modification of the chromic acid titration method. Soil Sci. 37 (1), 29–38.
Wang, L., Shi, Z.H., 2015. Size selectivity of eroded sediment associated with soil texture on steep slopes. Soil Sci. Soc. Am. J. 79 (3), 917.
Wang, Y.F., Xiao, X.M., 1993. Climatic gradient of main vegetation types in the Loess Plateau region. Acta Bot. Sin. 35, 291–299.
Wang, Z., Govers, G., Steegen, A., Clymans, W., Van den Putte, A., Langhans, C., Merckx, R., Van Oost, K., 2010. Catchment-scale carbon redistribution and delivery by water erosion in an intensively cultivated area. Geomorphology 124 (1–2), 65–74.
Wang, L., Shi, Z.H., Wang, J., Fang, N.F., Wu, G.L., Zhang, H.Y., 2014a. Rainfall kinetic energy controlling erosion processes and sediment sorting on steep hillslopes: a case study of clay loam soil from the Loess Plateau, China. J. Hydol. 512, 168–176.
Wang, X., Cammeraat, E.L.H., Cerli, C., Kalbitz, K., 2014b. Soil aggregation and the stabilization of organic carbon as affected by erosion and deposition. Soil Biol. Biochem. 72, 55–65.
Wei, X.R., Shao, M.A., 2007. Distribution of soil properties as affected by landforms in small watershed of loessial gully region. J. Nat. Resour. 22 (6), 946–953 (In Chinese).
Williams, J.R., Allmaras, R.R., Renard, K.G., Lyles, L., Moldenhauer, W.C., Langdale, G.W., Meyer, L.G., Rawls, W.J., Darby, G., Daniels, R., 1980. Soil erosion effects on soil productivity: a research perspective. J. Soil Water Conserv. 36 (2), 82–90.
Xu, G., Cheng, Y., Li, P., Li, Z., Zhang, J., Wang, T., 2015. Effects of natural rainfall on soil and nutrient erosion on sloping cropland in a small watershed of the Dan RiverChina. Quat. Int. 380–381, 327–333.
Zhang, G., Luo, R., Cao, Y., Shen, R., Zhang, X.C., 2010. Correction factor to dye-measured flow velocity under varying water and sediment discharges. J. Hydrol. 389 (1–2), 205–213.